5568–5577 Nucleic Acids Research, 2011, Vol. 39, No. 13 Published online 22 March 2011
doi:10.1093/nar/gkr141

Force-driven unbinding of proteins HU and Fis from DNA quantified using a thermodynamic Maxwell relation

Botao Xiao[1,2,*], Houyin Zhang[1], Reid C. Johnson[3,4] and John F. Marko[1,2]

[1]Department of Physics and Astronomy, [2]Department of Molecular Biosciences, Northwestern University, Evanston, IL 60208, USA, [3]Department of Biological Chemistry, David Geffen School of Medicine, and [4]Molecular Biology Institute, University of California, Los Angeles, CA 90095, USA

Received November 2, 2010; Revised February 8, 2011; Accepted February 24, 2011

ABSTRACT

Determining numbers of proteins bound to large DNAs is important for understanding their chromosomal functions. Protein numbers may be affected by physical factors such as mechanical forces generated in DNA, e.g. by transcription or replication. We performed single-DNA stretching experiments with bacterial nucleoid proteins HU and Fis, verifying that the force–extension measurements were in thermodynamic equilibrium. We, therefore, could use a thermodynamic Maxwell relation to deduce the change of protein number on a single DNA due to varied force. For the binding of both HU and Fis under conditions studied, numbers of bound proteins decreased as force was increased. Our experiments showed that most of the bound HU proteins were driven off the DNA at 6.3 pN for HU concentrations lower than 150 nM; our HU data were fit well by a statistical-mechanical model of protein-induced bending of DNA. In contrast, a significant amount of Fis proteins could not be forced off the DNA at forces up to 12 pN and Fis concentrations up to 20 nM. This thermodynamic approach may be applied to measure changes in numbers of a wide variety of molecules bound to DNA or other polymers. Force-dependent DNA binding by proteins suggests mechano-chemical mechanisms for gene regulation.

INTRODUCTION

A basic problem of DNA biochemistry is the monitoring of binding of proteins to the DNA double helix. Given that *in vivo* DNA is considered to be subjected to piconewton-scale mechanical forces (1,2), via the active machines that transcribe (3), replicate (4,5) and repair (6,7) the double helix, a logical question is how the binding of proteins to DNA is affected by DNA tension (8–10). The most likely proteins to be affected by DNA tension are those which bind most weakly, and these are typically proteins which bind non-specifically to essentially any sequence position along the double helix. In *Escherichia coli*, proteins of this type include histone-like protein from *Escherichia coli* strain U93 (HU) (11–14), factor for inversion stimulation (Fis) (15,16), integration host factor (IHF) (17,18) and histone-like nucleoid structuring protein (H-NS) (19–23), all of which are found in large quantities *in vivo* (tens of thousands of copies per cell in rapidly growing cells), and all of which help to fold and compact the nucleoid.

These four proteins all can compact DNA by bending it, or by stabilizing DNA–DNA nodes (i.e. non-covalent DNA–DNA contacts mediated by protein–DNA and/or protein–protein interactions), and therefore applied force can be expected to suppress their binding on general theoretical grounds. However, measuring this effect quantitatively is problematic. If one seeks to use fluorescent labeling, there is first the question of whether the labeling affects the binding affinity, and then the problem of calibration of the total fluorescence including the possible effects of changes in molecular brightness upon binding of a labeled protein to the double helix.

A further problem stems from the constraint that to apply calibrated forces to a DNA generally requires end-attachment of a particle. This constraint makes the use of total internal reflection fluorescence microscopy (TIRF) highly problematic, since it requires positioning of the fluorophores of interest less than ~200 nm from a surface (24), incompatible with the presence of a micron-sized end-attached particle. Alternative TIRF strategies using fluid flow to stretch molecules end-attached to a

*To whom correspondence should be addressed. Tel: +1 847 467 1187; Fax: +1 847 491 9982; Email: botaoshaw@hotmail.com
The authors wish it to be known that, in their opinion, the first two authors should be regarded as Joint First Authors.

surface apply inhomogeneous forces to DNA molecules (the tension must drop to zero at the free DNA end) (25). Non–TIRF strategies based on fluorescence require removal of protein in the surrounding bulk solution to avoid fluorescence background, and therefore can only make kinetic measurements that are out of thermodynamic equilibrium, since once protein is removed from bulk solution, one can expect gradual dissociation of initially DNA-bound molecules (13,15).

We recently proposed a new approach to the problem of determining the change in proteins or other small molecules bound to a DNA subjected to tension, using thermodynamics (8). A Gibbs adsorption isotherm equation was written in terms of the stretching force, the molecule extension, the chemical potential and bound protein numbers. A Maxwell relation was established relating these variables (8) whereby measurements of extension changes in response to changes in solution protein concentration may be used to infer changes in bound protein numbers induced by changes in applied force. Here, we report measurements of this type for non-specific binding of two of the most abundant DNA-bending proteins from *E. coli*, HU and Fis.

HU is a dimeric protein that binds to DNA in a largely sequence-independent manner (26–28). HU plays important roles in chromosome compaction, DNA replication, transcription and recombination processes (29,30). HU acts to compact DNA at physiological salt concentrations *in vitro* by introducing bends ranging from 53° to more than 140° in the DNA as assayed by X-ray crystallography, gel electrophoresis, DNA cyclization, atomic force microscopy and fluorescence resonance energy transfer (FRET). The bends introduced by HU are thought to be relatively flexible (12,27,31–36). The *in vivo* HU concentration has been reported to be 30 000 dimers per cell in exponential phase (37,38). Binding sites ranging from 6 to 42 bp in length have been measured under a variety of experimental conditions (35,39–42). The equilibrium constant (K_d) for non-specific binding of HU to DNA depends highly on salt concentration (13,41) and binding modes (11–13,40). For example, K_d values have been estimated to range from 400 nM at 15 mM NaCl (41), to 480 nM for non-cooperative binding at 150 mM NaCl (40), and to 29 μM for cooperative binding at 150 mM NaCl (40). No binding was observed in a recent experiment for HU concentrations of up to 500 nM at 300 mM NaCl (13).

Fis is also a dimeric nucleoid protein and is one of the most abundant DNA binding proteins in rapidly growing *E. coli* (30). Low concentrations (<100 nM) of Fis generally compact DNA under low mechanical tension *in vitro* (15). The bends in DNA induced by Fis dimer binding to different DNA segments have been measured to range from 50° to 90° with 65° overall curvature present in crystal structures (43–46). The minimum binding site was measured by gel-shift experiments and confirmed by crystallography to be ~21 bp per dimer (15,46). Fis binds non-specifically to DNA at low nanomolar concentrations, and increasing numbers of Fis associate with the Fis-DNA filaments at higher concentrations to form higher order looping complexes (15,16). Fis also acts as a specific regulator for a diverse group of DNA reactions, including transcription and recombination (30,47), and generally exhibits more sequence specificity in its DNA binding than HU. In the presence of excess DNA, Fis selectively binds to specific sites at K_d values ranging as low as 0.2 nM (43,44,46,48,49).

In this article we describe single-DNA-pulling experiments using HU and Fis under conditions where protein binding and unbinding are reversible. Given that previous studies have noted a breakdown of reversible binding for high protein concentrations (11,15), we first determine the ranges of protein concentrations and forces for which binding is reversible on laboratory timescales. We then analyze the force–extension data using our thermodynamic Maxwell relation approach (8). We find that both of these proteins have their binding destabilized by application of force to the double helix, i.e. their equilibrium binding constants are dependent on DNA tension.

MATERIALS AND METHODS

Protein expression and purification

Heterodimeric *E. coli* HU was purified from RJ5814 (*ihfB::cat fis::kan-767 endA*::Tn*10 his ilv* λ*cI857* N^+ containing pPL-*hupAB* from R. McMacken) by cation exchange chromatography on SP–Sepharose and FPLC mono S and FPLC gel filtration through Superose 75 (GE Healthcare LifeSciences) (13).

Wild-type *E. coli* Fis protein was overexpressed using the T7 promoter and purified from RJ3387 (*BL21 (DE3) fis::kan-767 endA8::tet*) as described (46).

Manipulation of DNA–protein complexes with magnetic tweezers

Two DNA substrates that bound HU and Fis non-specifically were used. The first, 48.5 kb λ DNA (Promega, Madison, WI, USA), was end-labeled with biotin and digoxygenin as described previously (50,51), and was used for studies of HU. The second, a 6.2 kb fragment from the linearized pFOS1 plasmid (New England Biolabs, Ipswich, MA, USA) was amplified by polymerase chain reaction (PCR) with two primers each labeled with biotin or digoxygenin, and was used for studies of Fis. Labeled pFOS1 fragment or λ DNA was incubated with 1.0 or 2.8 μm diameter streptavidin-coated paramagnetic beads (Dynabeads, Invitrogen, Grand Island, NY, USA) in phosphate-buffered saline (PBS) for 15 min. The bead-DNA constructs were later injected into a flow cell and tethered to a cover glass coated with anti-digoxygenin (Roche Diagnostics, Indianapolis, IN, USA). The flow cell was pre-incubated with 0.5 mg/ml bovine serum albumin (BSA) solution for 15 min to block non-specific interactions.

Vertical magnetic tweezers (MT) were constructed based on previous systems with slight modification as described (52,53). The vertical bead position was tracked by a piezoelectric objective positioner and the extension was determined using an automatic focusing algorithm. The transverse motion was captured by a camera and real time images were analyzed to calculate the force

between the paramagnetic bead and permanent magnets using a standard fluctuation technique (53,54). The force–extension (f–X) relationship of naked DNA was measured and compared with the worm-like chain model which is established to describe DNA mechanical properties, and for which the following approximate formula provides an accurate description (55):

$$f = \frac{k_B T}{A}\left[\frac{X}{X_0} + \frac{1}{4(1 - X/X_0)^2} - \frac{1}{4}\right]. \quad (1)$$

Here, k_B is Boltzmann's constant, T is the absolute temperature, $A \approx 50$ nm is the persistence length of a single DNA, and X_0 is the contour length of the DNA. All MTs experiments were performed at 25°C.

Force–extension measurements

Once a single DNA tether was calibrated, the PBS in the flow cell was substituted with the commonly used working buffers for proteins HU and Fis. The buffer for HU was composed of 20 mM HEPES, 150 mM NaCl, 0.5 mg/ml BSA, pH 7.5 (13). The buffer for Fis contained 20 mM HEPES, 100 mM K-glutamate, 0.5 mM EDTA and 0.5 mg/ml BSA, pH 7.5 (15,16). Three hundred microliter of solution was used for the ~60 µl flow cell. During this solution exchange process and later ones, the force applied to the DNA tether was held at ~2 pN to prevent it from sticking to the cover glass. Extension of the λ DNA or pFOS1 fragment at a given force (from 0.05 to 12 pN) was measured using the automatic focusing algorithm in the working buffer and protein solutions with attention paid to making sure the DNA–protein complex length had stabilized.

In addition to the automatic focusing method, a much faster extension measurement method (15,53) was also used for the shorter pFOS1 fragment. Briefly, after an automatic focusing measurement, the power spectra of images of both the surface-bound bead and the DNA bead were obtained. The spectrum at an empirically determined wave number changes monotonically with bead position, and can be used as a measurement of bead position. The dynamic DNA-bead spectrum was compared with the reference to determine the DNA extension. This allowed extension measurements to be performed 100 times per second, much faster than the automatic focusing method (~10 per min).

Maxwell relation and calculation of changes in protein numbers

For proteins binding onto a single-stretched DNA, the differential for the thermodynamic potential E can be described in terms of a Gibbs adsorption isotherm:

$$-\mathrm{d}E = \mathrm{d}(k_B T \ln Z) = \langle X\rangle \mathrm{d}f + \langle N\rangle \mathrm{d}\mu, \quad (2)$$

$$\mu = k_B T \ln\left(\frac{c}{c_0}\right). \quad (3)$$

Here, X is the end-to-end extension of the DNA in the force direction. N is the number of bound proteins, μ is the protein chemical potential, and where c is the protein concentration (the logarithmic dependence of µ on c applies to low-concentration solutions, the case of interest here). For the moment, the constant c_0 is undetermined: it simply additively shifts the protein chemical potential, and mainly provides a way to make the inside of the logarithm dimensionless. However, in a microscopic model c_0 controls the binding affinity of a protein to a DNA binding site (see below) (9). The averages emphasize that the respective quantities, i.e. $\langle X\rangle$ and $\langle N\rangle$, should be measured in equilibrium. The partial derivatives of $\ln Z$ give rise to the average end-to-end extension and the average bound protein number:

$$\langle X\rangle = \left(\frac{\partial k_B T \ln Z}{\partial f}\right)_\mu, \ \langle N\rangle = \left(\frac{\partial k_B T \ln Z}{\partial \mu}\right)_f. \quad (4)$$

Barring any singularities, the mixed second derivatives are independent of the order of partial differentiation. This generates an analog of the Maxwell relation of classical thermodynamics:

$$\left(\frac{\partial\langle X\rangle}{\partial\mu}\right)_f = \left(\frac{\partial\langle N\rangle}{\partial f}\right)_\mu. \quad (5)$$

We denote this quantity as the 'mixed derivative'; the term to the left is the variation of extension with concentration in units of nm/k_BT, which can be measured; the term to the right is the variation of bound protein number with force.

For the f–X measurements at fixed μ in equilibrium state, the change in number of bound proteins as force is changed from f_0 to f_i can be obtained by integration:

$$\langle N_i\rangle - \langle N_0\rangle = \int_{f_0}^{f_i} df\left(\frac{\partial\langle X\rangle}{\partial\mu}\right)_f. \quad (6)$$

For proteins that compact DNA (such as HU and Fis at sufficiently low concentrations), extension goes down with increased protein concentration, making the right-hand side of Equation (6) negative. In turn, this indicates that as force is increased, the number of proteins bound to a DNA molecule will decrease.

We note that the 'number of proteins' N refers to the number of independently binding entities. In the case where the proteins bind as dimer units which are pre-formed and are highly stable in solution, N therefore reflects the number of dimers bound; in this case the concentration c refers to the dimer concentration. This actually is the case for the proteins HU and Fis studied in this article.

Model calculation to describe HU–DNA interactions

We use a recently developed discrete semiflexible polymer model (8,9,56,57) to describe results for experiments with HU. Briefly, the DNA molecule is treated as a polymer made up of a series of segments, each of which has a potential protein binding site. A protein can bind to the node between any two adjacent segments. The free energy of the

protein–DNA complex is expressed as a sum over these segments:

$$\frac{F}{k_BT} = \sum_{i=1}^{N} \left\{ \frac{a}{2} |\hat{t}_{i+1} - \hat{t}_i|^2 (1 - n_i) + \left[\frac{a'}{2} \left(\hat{t}_{i+1} \cdot \hat{t}_i - \gamma \right)^2 - \ln \frac{c}{c_0} \right] n_i - \frac{bf}{k_BT} \hat{t}_i \cdot \hat{x} \right\}, \quad (7)$$

where b is the segment length, which corresponds to the binding site size; N is the number of segments, $N = X_0/b$ [X_0 is the contour length of the DNA, see Equation (1)]; $\hat{t}_i$ is the unit vector, which defines the direction of each segment; a is the naked DNA bending rigidity, $a = A/b$; a' is the protein–DNA bending rigidity and is dimensionless; n_i is the protein occupation degree of freedom, which is either 0 for unoccupied node or 1 when a protein is bound to this node; θ is the preferred bending angle between adjacent segment caused by protein binding, $\cos(\theta) = \gamma$; f is the applied force; the unit vector $\hat{x}$ is the direction of applied force (57). The bulk protein concentration c enters into the model via the free energy difference between free and bound protein.

The one remaining parameter c_0 needs to be set by comparison with experiment. With other parameters (a, a', θ, b, N, etc.) fixed, different c_0 values will generate different force–extension curves. We fit the theoretical model to the experimental data by minimization of χ^2 between theoretical and experimental extensions as a function of force:

$$\chi^2(c_0) = \sum_{i=1}^{N_{\text{data}}} \frac{[X_i(c_i, f_i) - R_x(c_0; c_i, f_i)]^2}{\delta_i^2}. \quad (8)$$

Here, N_{data} is the total number of experimental data, and δ_i is the uncertainty of the HU–DNA extension measured at force f_i and HU concentration c_i. R_x (c_0; c_i, f_i) is the HU–DNA extension calculated from the model for different c_0 at force f_i and HU concentration c_i. Error for the fit value of c_0 was estimated from the range over which the change in χ^2 was less than N_{data}. The K_d is the concentration at which 50% of the protein binding sites are occupied at zero applied force, which was determined from numerical calculations for the Boltzmann equilibrium for Equation (7) using the fit value for c_0. Although c_0 has the dimension of a dissociation constant, differences in free energy for protein-bound and -unbound segments shift K_d away from c_0.

We used a transfer matrix method to calculate the equilibrium partition function, which was used to obtain the force–extension relationship. The DNA segment length b (corresponding to the HU binding site size) was chosen to be 7 nm based on available structural data (34). The bending rigidity a' was chosen to be a small value in terms of the observation of flexible hinge behavior of HU–DNA binding (12), e.g. $a' = 1$. The preferred bending angle θ was chosen to be 90°, a value in the midrange of previous reports (12,31–34). For the model, numbers of proteins bound to the DNA could be directly computed; it was checked that changes in bound HU numbers obtained from direct theoretical model calculation agreed with those obtained from the Maxwell relation [Equation (6)].

RESULTS

Single-DNA tethers were identified, and a sample of fits to the worm-like chain model [Equation (1)] for naked DNA are provided in Supplementary Figure S1. No difference among *f–X* curves was observed in PBS and in the buffers for proteins HU and Fis (Supplementary Figure S2). *f–X* curves at a given protein concentration were measured to calculate the changes in bound protein numbers.

Verification that *f–X* measurements were in thermodynamic equilibrium

To use the Maxwell equation to analyze the DNA stretching experiments, the *f–X* measurements must be in thermodynamic equilibrium. Whether the force was increased from 0.05 to 12 pN, or vice versa, the *f–X* curves at a given protein solution were observed to be the same, i.e. there was no hysteresis. As shown in Figure 1A, the *f–X* curves of HU-λ DNA shifted within 10 min when the HU concentrations increased from 0 to 100 nM, then to 500 nM. One hour after replacing the high concentration solution (500 nM) with the lower one (100 nM), the *f–X* curve (100 nM return) overlaid with the curve obtained at previous 100 nM HU; thus there was no hysteresis observed resulting from HU concentration changes. Reversibility for other force and HU concentration ranges are shown in Supplementary Figure S3A.

Similarly, the *f–X* curves for Fis-pFOS1 fragment complexes (Figure 1B) shifted within 10 min when the Fis concentrations increased from 0 to 10 nM and then to 28 nM. Three hours after changing the high concentration solution (28 nM) to the lower one (10 nM), the *f–X* curve (10 nM return) returned to the same as the original *f–X* curve for 10 nM. The dissociation process monitored via change in extension in 10 nM Fis solution is shown in Supplementary Figure S4. Reversibility for other force and Fis concentration ranges is shown in Supplementary Figure S3B. These results demonstrate that the equilibrated *f–X* curves depended only on the final state of the system but not on the history of the solution, i.e. thermodynamic equilibrium could be reached.

HU force–extension curves

We next carried out *f–X* measurements for a series of protein concentrations, which were 25, 50, 100, 150, 250, 375 and 500 nM for HU (Figure 2A, dots; some data points not shown for the sake of clarity). As HU concentration was raised, the extension of HU–DNA complexes at a certain force reduced progressively. The difference between HU–DNA and naked λ DNA shrank as force was increased. The maximum compaction ratio at 0.1 pN was ~49%. The measured *f–X* curves increasingly shifted to higher forces as the protein concentrations increased. Fits to the worm-like chain model [Equation (1)] for HU–DNA complexes were performed (Supplementary Figure S1). The apparent persistence

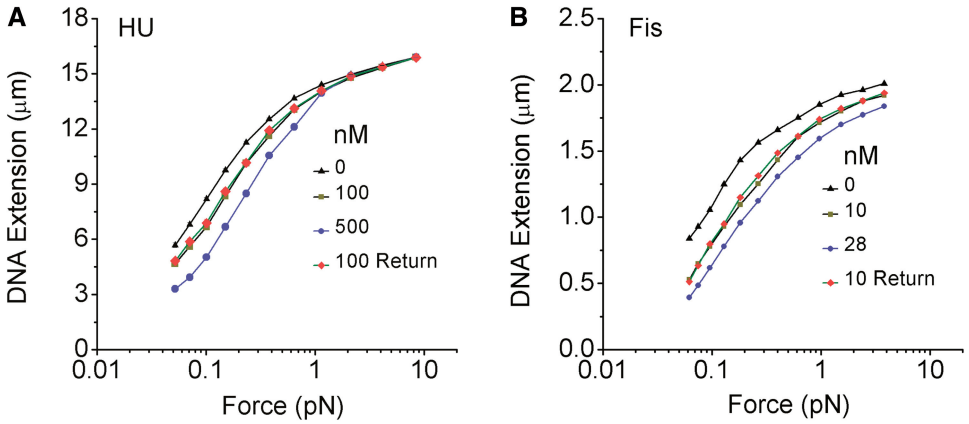

Figure 1. Thermodynamic equilibrium of *f–X* measurements. (**A**) Reversibility of HU-λ DNA binding demonstrated via *f–X* curves. DNA extension decreased when HU concentration was increased from 0 to 100 nM, and then to 500 nM. One hour after replacing the 500 nM HU solution with 100 nM HU solution, the *f–X* curve of '100 return' overlaid with the curve previously obtained at 100 nM HU, indicating reversibility of binding. Each experimental data point, presented as the mean value with error bars (SE), was obtained from 15 to 20 separate measurements. The errors range from 6 nm at 8.4 pN to 0.15 μm at 0.05 pN. (**B**) Reversibility of Fis-pFOS1 fragment binding. As the Fis concentration was cycled up and down, the *f–X* curves shifted right and left. The curve of '10 return' was the same as the previous 10 nM curve. Each experimental data point, presented as the mean value with error bars (SE), was obtained from 3700 to 4300 separate fast extension measurements. The errors range from 3 nm at 3.8 pN to 0.03 μm for 0.06 pN.

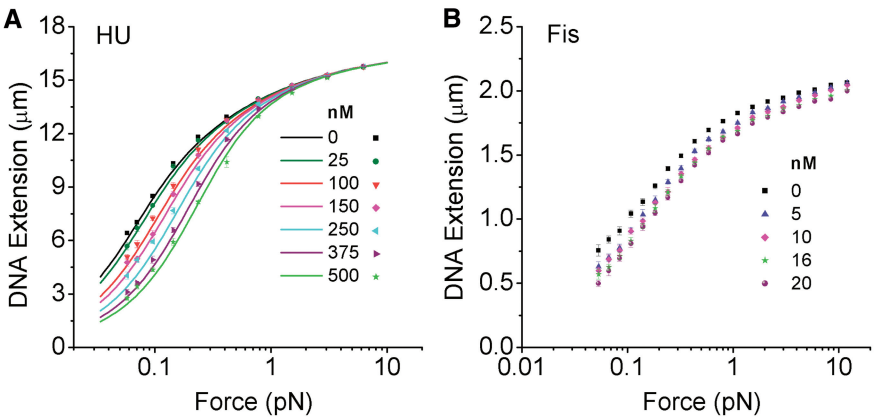

Figure 2. *f–X* curves of protein–DNA complexes. Each experimental data point, presented as the mean value with error bars (SE), was obtained from 6 to 10 separate measurements. Successively higher concentrations led to more protein binding, and consequently more compaction against the applied force. *f–X* curves shifted right as the added protein concentrations were increased. (**A**) HU-concentration dependence of *f–X* curves of a λ DNA. Model calculations (lines) from Equation (7) fit the experimental data (dots) well. (**B**) Fis-concentration dependence of *f–X* curve of a pFOS1 fragment.

length of DNA decreased from 49 ± 2 to 22 ± 1 nm as the HU concentrations increased from 0 to 500 nM.

Model force–extension curves for HU–DNA complexes

f–X curves of HU–DNA complexes were computed using the discrete semiflexible polymer model [Equation (7)] (57). Parameters for the calculations were chosen using published estimates of HU–DNA binding site size and bending angle ('Materials and Methods' section). The parameter c_0 was determined by the fitting of experimental force–extension data [Equation (8)] and was found to be 18 ± 5 μM, corresponding to an effective K_d of 1.6 ± 0.5 μM. Model calculations of *f–X* curves for HU concentrations used in our experiments, i.e. 0, 25, 50, 100, 150, 250, 375 and 500 nM, were demonstrated as the lines in Figure 2A (50 nM not shown for the sake of clarity). The *f–X* curves increasingly shifted to a higher force regime as the protein concentrations increased, agreeing well with the experimental data.

Fis force–extension curves

f–X curves were also obtained for a set of Fis concentrations, i.e. 3, 5, 8, 10, 12, 14, 16, 18 and 20 nM, for 6.2 kb pFOS1 DNA tethers (Figure 2B; some data points not shown for the sake of clarity). For higher concentrations of Fis, nonequilibrium effects (irreversibility) were observed, making a thermodynamic approach to estimation of protein numbers impossible. The extension of Fis-DNA complexes at a given force decreased as Fis concentration was raised. Compared to the HU experiments, the difference between Fis-DNA and naked DNA did not shrink much as force was increased. At 0.1 pN, the

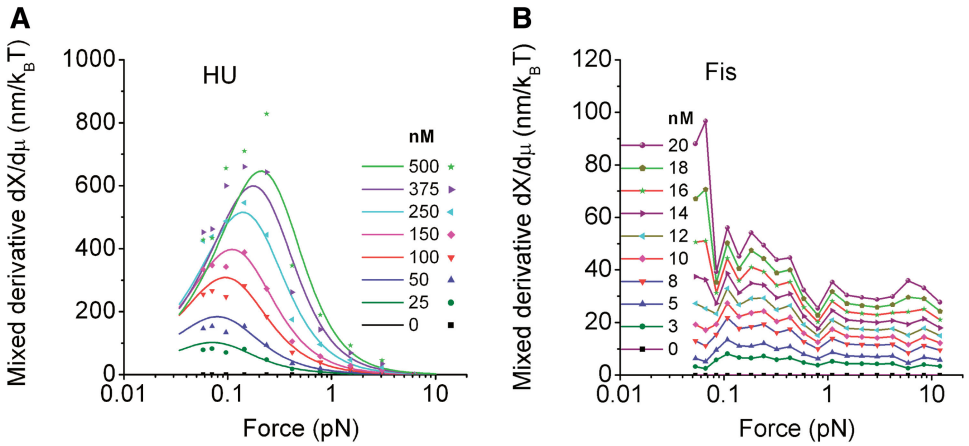

Figure 3. Mixed derivatives as a function of force. The mixed derivatives increased as the protein concentrations increased. (**A**) $dz/d\mu$ for HU calculated from experimental data and the model. A peak value appeared at a low force region (~0.2 pN), followed by general trends of decrease. Model calculations (lines) agreed with the experimental HU data (dots). (**B**) $dz/d\mu$ for Fis calculated from experimental data. The mixed derivatives decreased as the force increased.

maximum compaction ratio was ~25% for Fis. The persistence length of DNA decreased from 50 ± 2 to 37 ± 1 nm as the Fis concentrations increased from 0 to 20 nM.

Mixed derivative for HU and Fis

Mixed derivatives were calculated from the *f*–*X* experimental data according to Equation (5) and were plotted versus force (Figure 3). The mixed derivatives increased as the protein concentrations increased. For the HU experimental data, a peak value appeared at ~0.2 pN, followed by general trends of decrease (Figure 3A, dots).

Model calculations of mixed derivatives of HU obtained from the fit of force–extension data are compared with data in Figure 3A. These calculations agreed well with the experimental results; in particular the shape and location of the peak in the mixed derivative closely matches that obtained from analysis of experimental data.

For the Fis experimental data, the mixed derivatives decreased as a function of the force (Figure 3B), and did not show the broad peak observed in the HU data. In general the smaller amount of compaction driven by Fis over the concentration range we were able to study led to less accurate determination of the mixed derivative, but still it is clear that the shape of the mixed derivative for Fis–DNA interactions is very different from that for HU–DNA interactions.

Changes in bound HU number

Integrating the mixed derivatives over force gives rise to the changes of bound protein numbers [Equation (6)]. For λ DNA and HU, the loss of protein numbers increased and reached a plateau as the forces increased from 0.06 to 6.3 pN (Figure 4A, dots). The total number of HU dimers driven off DNA over this force range added up to 610 ± 20 for an HU concentration of 500 nM. Therefore, increases of force from 0.06 to 6.3 pN can lead to a decrease of approximately one HU dimer per 80 bp when the bulk HU concentration is 500 nM.

Model calculation of changes in bound HU number

Changes in bound protein numbers were also calculated for HU using the model. For λ DNA and HU, the loss of protein numbers increased as force increased from 0 to 6.3 pN (Figure 4A, lines). Considering the 500 nM HU concentration case, the total number of proteins lost over this force range was 520. Thus, for 500 nM HU, an increase of force from 0 to 6.3 pN leads to a total decrease of approximately one HU dimer per 93 bp, which corresponds to removal of most of the proteins that are bound at zero force. Overall, the model calculations agreed well with the HU experimental results.

Results of the model were not highly sensitive to small changes in *b* as long as it was between 3 and 10 nm. Similarly, changes of a' did not strongly modify the results. However, c_0 needs to be set for each choice of a' and *b*, mainly because of shifts in the net free energy of the HU–DNA complex introduced by modification of binding site size and HU–DNA complex flexibility. However, after this adjustment, we found that the observed K_d (50% binding site occupation concentration) was nearly unchanged: for a' in the range of 0–10 and *b* in the range of 5–10 nm, the K_d shifted very little, remaining in the range 1.3–2.1 μM. Given that we consider a', *b* and θ to be set by previous experiments, the only fit parameter is c_0, which we have adjusted to obtain theoretical force–extension curves that resemble the experiment (Figure 2A). Thus the model provides a rather robust estimate of the net K_d of HU for DNA in our solution conditions, of ~1.6 ± 0.5 μM.

Changes in bound Fis number

For 6.2 kb pFOS1 fragment and Fis, the loss of proteins increased as the forces increased but no saturation was observed in the force and concentration ranges studied.

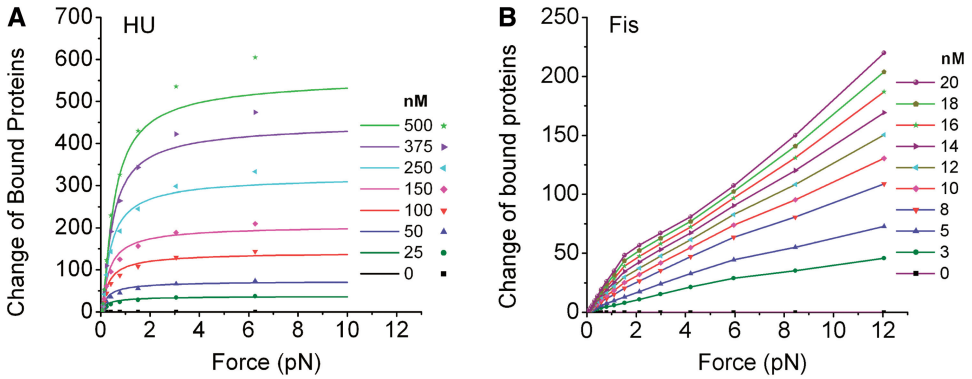

Figure 4. Changes of protein numbers on a single stretched DNA molecule. For the binding of HU or Fis under conditions where they compacted DNA, proteins were released from DNA as force was increased. (**A**) Changes of HU numbers. In experiments (dots), the loss of proteins on a λ DNA increased as the forces increased from 0.06 to 6.3 pN, and as the HU concentrations increased from 25 to 500 nM. In the model calculation (lines), the loss of proteins increased smoothly and reached a plateau as the forces increased from 0 to 6.3 pN. For 500 nM HU, the loss of proteins number was 520 from model calculation, and 610 from experiments. (**B**) Changes of Fis numbers calculated from experimental data. The loss of proteins on a 6.2 kb pFOS1 fragment increased to 220 dimers for the 20 nM Fis experiment as the forces increased from 0.05 to 12.0 pN. No saturation was observed in the force and concentration ranges.

In other words, the numbers of bound proteins increased continuously as the forces decreased over the range studied. Changes of Fis numbers at 20 nM bulk concentration were 110 ± 10 from 0.05 to 6.0 pN, and 220 ± 20 from 0.05 to 12.0 pN (Figure 4B), a loss of one dimer for about every 28 bp.

DISCUSSION

We have measured the changes of *E. coli* nucleoid protein numbers on a single DNA molecule using a thermodynamic approach, employing a Maxwell relation that relates extension change with protein concentration to change in protein binding with force. The DNA-bending proteins HU and Fis compact DNA when they bind under the conditions used here; therefore when thermal equilibrium can be reached, increased force can be expected to drive these proteins to dissociate. However, determining exactly how many proteins are driven off a DNA in a solution containing a relatively high concentration of protein is problematic. The thermodynamic approach taken in this article provides a tool that is complementary to technically challenging molecule-counting methods (e.g. quantitative fluorescence measurements). Although only changes in numbers of bound protein can be measured [see Equation (6)], our thermodynamic approach is technically straightforward, and uses only small amounts of native (unlabeled) protein.

Force can pull off a fraction of bound DNA-bending proteins

If the binding site for HU is estimated to be 21 bp per dimer, based on co-crystal structures (34), the maximum number of bound HU on λ DNA would be ~2300 dimers. However, our experiments have been done at HU concentrations well below the K_d: our experiments at 500 nM HU are ~3-fold below the K_d we estimate using our microscopic model. With 500 nM HU in solution, as force is increased from 0.06 to 6.3 pN, we find that about one quarter of the HUs that could possibly bind (610 of 2300 proteins) can be driven off a DNA molecule by tension. Comparison with our model (Figure 4A) indicates that in fact, the ~600 proteins driven off consist of the bulk of the proteins that are bound at zero force. Therefore, we find that for lower bulk HU concentrations (<150 nM), most of the bound HU can be pushed off the DNA by a force of 6.3 pN. At higher HU concentrations, however, a small fraction of proteins can remain bound to the DNA at 6.3 pN, suggested by the fact that the extension of HU–DNA complexes at high protein concentrations and high force does not quite equal the extension of naked DNA.

We emphasize that our Maxwell relation analysis monitors the change in HU dimers bound to DNA, and not just straightening of the HU–DNA complexes by force. In previous non-equilibrium experiments we noted that rather small increases in force at the subpiconewton level (0.1 and 0.3 pN) substantially enhance the dissociation rate of HU from DNA (13). The present study establishes that not only dissociation, but also equilibrium binding of HU to DNA in protein-containing solution is DNA-tension dependent.

For Fis, in the concentration range and buffer conditions we have studied (<20 nM, 100 mM univalent salt), each bound dimer occupies roughly 21 bp (15,46), indicating that the 6.2 kb pFOS1 fragment can absorb a maximum of 295 Fis dimers in this binding mode. Gel shift experiments indicate that at 20 nM Fis concentration, most if not all of these Fis binding sites along a DNA are occupied (15). The maximum changes of protein numbers observed in our experiment (in a solution of 20 nM Fis) are consistent with this, in that they are less than this limit. Over a force range of 0.05–12 pN, we estimate that ~220 Fis dimers can be pulled off a DNA in 20 nM Fis solution. The lack of a plateau behavior in the total number of proteins driven off with force (Figure 4B) indicates that more Fis molecules can be driven off DNA by higher forces than we have used in this study.

Following our theoretical proposal of the Maxwell relation approach to measuring protein binding changes (8) and during the preparation of this article, Liebesny *et al.* (58) reported experiments similar to those reported here, for binding of λ repressor to DNA. For non-specific binding of that protein to a 15.5 kb DNA, Liebesny *et al.* found that over a force range of 0.13–4.81 pN, roughly 138 proteins were released. These results are reasonable, and we anticipate that our approach will be useful for monitoring binding of a wide variety of proteins to DNA.

We emphasize, that the Maxwell relation method hinges on being in thermodynamic equilibrium, and without demonstration of the ability to cycle the force–extension curves reversibly over the concentration and force ranges of interest (Figure 1), use of the Maxwell relation to infer changes in bound protein number is questionable. We have observed numerous non-equilibrium effects in DNA–protein interaction studies (11,15). In general use of low salt or high protein concentration leads to formation of complexes which are unable to disassemble spontaneously or which show very slow off-kinetics (11,13,15); we have found that the salt and protein concentration thresholds for the onset of non-equilibrium effects vary from protein to protein, with some proteins showing very slow unbinding kinetics even in physiological buffers. It is essential that before using the methods described in this article one verifies thermal equilibration of protein–DNA interactions (Figure 1).

A previous theoretical study predicted that any protein that compacts DNA may have its binding destabilized by application of force to the double helix (9). We subsequently experimentally observed that increasing tension even at sub-piconewton levels significantly accelerated dissociation of HU from DNA (13). These results taken together indicate that the equilibrium binding constants for DNA-bending proteins are DNA-tension-dependent, with significant effects below 1 pN. Our results are consistent with the previous work of Vladescu *et al.* (59) on small molecule DNA intercalating agents. In the cell, this provides a mechanism for remodeling of *E. coli* chromosome structure: tension generated in DNA on the few pN scale, e.g. by transcription, will result in dissociation of chromosome-folding proteins such as HU and Fis, further opening up DNA for access by the transcription machinery.

We also note that for proteins which lengthen the DNA double helix, the binding affinity can be expected to be increased by applied tension (9); our Maxwell relation approach can be used in this case as well, but in this case the bound protein number will be observed to increase with force at fixed bulk protein concentration.

Utility and limitations of the semiflexible polymer model for DNA-bending proteins

The calculations using our discrete semiflexible polymer model (57) agreed generally well with the experimental data of HU–DNA complexes. The discrepancy at high HU concentration could be caused by the inhomogeneous binding behaviors of HU (11–13,39–41), such as cooperative binding, which were not taken into account in the model. The HU–DNA interactions for our experimental conditions can be described well by experimental-data-dictated choices of parameters in the model, i.e. binding site size, bending angle and bending rigidity. The close agreement between this model and our data gives us considerable confidence that HU is bending DNA in our experiments and binding in a mainly non-specific manner, and that our Maxwell relation estimates of force-induced dissociation of proteins are reasonable.

On the other hand, we have found that our microscopic semiflexible model does not work well to describe the Fis-DNA force–extension data. We emphasize that this does not invalidate our Maxwell relation analysis. Instead, this indicates that Fis–DNA interactions are microscopically more complex than can be described by a uniform binding and bending mechanism. Fis is known to form higher order filaments by protein–protein interactions that result in DNA compaction and looping (15,16). However, these binding modes occur at higher Fis concentrations than employed in this work. A more likely explanation is that Fis does not bind DNA in an entirely sequence-neutral manner. Instead, Fis exhibits a continuum of binding affinities with K_ds beginning at the subnanomolar level (46,48) along with a range of bending angles that are influenced by the sequences flanking the core binding site (43,44). Fis acts as a specific regulator for a diverse group of DNA reactions, including transcription and recombination (30,47). In these roles Fis stably binds to specific sites that are related by a highly degenerate 15 bp DNA sequence (48,49,60,61). Recent genome-wide binding studies have identified 1000–1500 sites within the *E. coli* chromosome that are specifically bound by Fis (61,62). Thus, Fis exhibits considerably more sequence-specificity in its DNA binding than HU. Biophysical evidence that multiple populations of Fis-bound complexes exist is suggested by the inability of applied force to bring a DNA molecule back to its naked length [see high force region in Figures 1B and 2B, see also Figure 3B of Skoko *et al.* (15)]. Inhomogeneous binding effects might be incorporated in a more complex model (with more parameters), but we leave this for a future study.

Maxwell relations for binding of ligands to flexible objects have a wide range of applications

The Maxwell relation (8) is a practical approach to measure the changes of bound protein numbers on a single DNA molecule under tension. The same approach may be applied to measure the change in numbers of bound molecules binding to other polymers by investigators in different fields of research. For instance, a possible application in cell biology is determination of how many proteins are bound to an actin filament as a function of tension on it (63–65). Another application of the general approach that has recently been discussed is determination of the quantity of glucose binding to a polyallylamine (66). A slightly different Maxwell relation discussed in our previous article (8) has also been adopted to estimate the effective torsional modulus and the buckling torque of

DNA (67), and a third form has been used to estimate the adsorption site lengths and the association constants of molecules in solution binding to a synthetic polymer (66). Finally, the same general approach used in this article could be used to monitor binding or unbinding of proteins to DNA driven by torsional stress (supercoiling) (8). All of these disparate experimental measurements are unified by the same general approach based on classical thermodynamic Maxwell relations.

SUPPLEMENTARY DATA

Supplementary Data are available at NAR Online.

ACKNOWLEDGEMENTS

We thank Dr Hua Bai, Dr John Graham, Prof. Jie Yan and Dr Dan Grilley, for technical assistance and helpful discussions; Jenna McCracken for help with HU purification; and Dr Stefano Stella for Fis purification.

FUNDING

Work in the JFM lab was supported by the National Science Foundation (DMR-0715099, PHY-0852130, DMR-0520513), by the National Institutes of Health [U54CA143869-01 (NU-PS-OC)] and by the Chicago Biomedical Consortium with support from the Searle Funds at the Chicago Community Trust. Work in the RCJ lab was supported by National Institutes of Health [GM038509]. Funding for open access charges: National Science Foundation (PHY-0852130).

Conflict of interest statement. None declared.

REFERENCES

1. Bustamante,C., Bryant,Z. and Smith,S.B. (2003) Ten years of tension: single-molecule DNA mechanics. *Nature*, **421**, 423–427.
2. Woldringh,C.L. (2002) The role of co-transcriptional translation and protein translocation (transertion) in bacterial chromosome segregation. *Mol. Microbiol.*, **45**, 17–29.
3. Yin,H., Wang,M.D., Svoboda,K., Landick,R., Block,S.M. and Gelles,J. (1995) Transcription against an applied force. *Science*, **270**, 1653–1657.
4. Stano,N.M., Jeong,Y.J., Donmez,I., Tummalapalli,P., Levin,M.K. and Patel,S.S. (2005) DNA synthesis provides the driving force to accelerate DNA unwinding by a helicase. *Nature*, **435**, 370–373.
5. Wuite,G.J., Smith,S.B., Young,M., Keller,D. and Bustamante,C. (2000) Single-molecule studies of the effect of template tension on T7 DNA polymerase activity. *Nature*, **404**, 103–106.
6. Kowalczykowski,S.C. (2008) Structural biology: snapshots of DNA repair. *Nature*, **453**, 463–466.
7. Dillingham,M.S. and Kowalczykowski,S.C. (2008) RecBCD enzyme and the repair of double-stranded DNA breaks. *Microbiol. Mol. Biol. Rev.*, **72**, 642–671.
8. Zhang,H. and Marko,J.F. (2008) Maxwell relations for single-DNA experiments: Monitoring protein binding and double-helix torque with force-extension measurements. *Phys. Rev. E Stat. Nonlin. Soft Matter Phys.*, **77**, 031916.
9. Yan,J. and Marko,J.F. (2003) Effects of DNA-distorting proteins on DNA elastic response. *Phys. Rev. E Stat. Nonlin. Soft Matter Phys.*, **68**, 011905.
10. Marko,J.F. and Siggia,E.D. (1997) Driving proteins off DNA using applied tension. *Biophys. J.*, **73**, 2173–2178.
11. Skoko,D., Wong,B., Johnson,R.C. and Marko,J.F. (2004) Micromechanical analysis of the binding of DNA-bending proteins HMGB1, NHP6A, and HU reveals their ability to form highly stable DNA-protein complexes. *Biochemistry*, **43**, 13867–13874.
12. van Noort,J., Verbrugge,S., Goosen,N., Dekker,C. and Dame,R.T. (2004) Dual architectural roles of HU: formation of flexible hinges and rigid filaments. *Proc. Natl Acad. Sci. USA*, **101**, 6969–6974.
13. Xiao,B., Johnson,R.C. and Marko,J.F. (2010) Modulation of HU-DNA interactions by salt concentration and applied force. *Nucleic Acids Res.*, **38**, 6176–6185.
14. Schnurr,B., Vorgias,C. and Stavans,J. (2006) Compaction and supercoiling of single, long DNA molecules by HU protein. *Biophys. Rev. Lett.*, **1**, 29–44.
15. Skoko,D., Yoo,D., Bai,H., Schnurr,B., Yan,J., McLeod,S.M., Marko,J.F. and Johnson,R.C. (2006) Mechanism of chromosome compaction and looping by the *Escherichia coli* nucleoid protein Fis. *J. Mol. Biol.*, **364**, 777–798.
16. Skoko,D., Yan,J., Johnson,R.C. and Marko,J.F. (2005) Low-force DNA condensation and discontinuous high-force decondensation reveal a loop-stabilizing function of the protein Fis. *Phys. Rev. Lett.*, **95**, 208101.
17. Ali,B.M., Amit,R., Braslavsky,I., Oppenheim,A.B., Gileadi,O. and Stavans,J. (2001) Compaction of single DNA molecules induced by binding of integration host factor (IHF). *Proc. Natl Acad. Sci. USA*, **98**, 10658–10663.
18. Sugimura,S. and Crothers,D.M. (2006) Stepwise binding and bending of DNA by *Escherichia coli* integration host factor. *Proc. Natl Acad. Sci. USA*, **103**, 18510–18514.
19. Liu,Y., Chen,H., Kenney,L.J. and Yan,J. (2010) A divalent switch drives H-NS/DNA-binding conformations between stiffening and bridging modes. *Genes Dev.*, **24**, 339–344.
20. Amit,R., Oppenheim,A.B. and Stavans,J. (2003) Increased bending rigidity of single DNA molecules by H-NS, a temperature and osmolarity sensor. *Biophys. J.*, **84**, 2467–2473.
21. Stavans,J. and Oppenheim,A. (2006) DNA-protein interactions and bacterial chromosome architecture. *Phys. Biol.*, **3**, R1–10.
22. Dame,R.T., Noom,M.C. and Wuite,G.J. (2006) Bacterial chromatin organization by H-NS protein unravelled using dual DNA manipulation. *Nature*, **444**, 387–390.
23. Dame,R.T., Wyman,C. and Goosen,N. (2000) H-NS mediated compaction of DNA visualised by atomic force microscopy. *Nucleic Acids Res.*, **28**, 3504–3510.
24. Reck-Peterson,S.L., Derr,N.D. and Stuurman,N. (2010) Imaging single molecules using total internal reflection fluorescence microscopy (TIRFM). *Cold Spring Harb. Protoc.*, **2010**, pdb top73.
25. Doyle,P.S., Ladoux,B. and Viovy,J.L. (2000) Dynamics of a tethered polymer in shear flow. *Phys. Rev. Lett.*, **84**, 4769–4772.
26. Swinger,K.K. and Rice,P.A. (2007) Structure-based analysis of HU-DNA binding. *J. Mol. Biol.*, **365**, 1005–1016.
27. Hodges-Garcia,Y., Hagerman,P.J. and Pettijohn,D.E. (1989) DNA ring closure mediated by protein HU. *J. Biol. Chem.*, **264**, 14621–14623.
28. Grove,A. (2010) Functional evolution of bacterial histone-like HU proteins. *Curr. Issues Mol. Biol.*, **13**, 1–12.
29. Oberto,J., Nabti,S., Jooste,V., Mignot,H. and Rouviere-Yaniv,J. (2009) The HU regulon is composed of genes responding to anaerobiosis, acid stress, high osmolarity and SOS induction. *PLoS One*, **4**, e4367.
30. Johnson,R.C., Johnson,L.M., Schmidt,J.W. and Gardner,J.F. (2005) In Higgins,N.P. (ed.), *The Bacterial Chromosome*. ASM Press, Washington DC, pp. 65–132.
31. Kamashev,D., Balandina,A. and Rouviere-Yaniv,J. (1999) The binding motif recognized by HU on both nicked and cruciform DNA. *EMBO J.*, **18**, 5434–5444.
32. Lavoie,B.D., Shaw,G.S., Millner,A. and Chaconas,G. (1996) Anatomy of a flexer-DNA complex inside a higher-order transposition intermediate. *Cell*, **85**, 761–771.
33. Sagi,D., Friedman,N., Vorgias,C., Oppenheim,A.B. and Stavans,J. (2004) Modulation of DNA conformations through the formation of alternative high-order HU-DNA complexes. *J. Mol. Biol.*, **341**, 419–428.

34. Swinger,K.K., Lemberg,K.M., Zhang,Y. and Rice,P.A. (2003) Flexible DNA bending in HU-DNA cocrystal structures. *EMBO J.*, **22**, 3749–3760.
35. Wojtuszewski,K. and Mukerji,I. (2003) HU binding to bent DNA: a fluorescence resonance energy transfer and anisotropy study. *Biochemistry*, **42**, 3096–3104.
36. Paull,T.T., Haykinson,M.J. and Johnson,R.C. (1994) HU and functional analogs in eukaryotes promote Hin invertasome assembly. *Biochimie*, **76**, 992–1004.
37. Azam,T.A., Iwata,A., Nishimura,A., Ueda,S. and Ishihama,A. (1999) Growth phase-dependent variation in protein composition of the *Escherichia coli* nucleoid. *J. Bacteriol.*, **181**, 6361–6370.
38. Dixon,N.E. and Kornberg,A. (1984) Protein HU in the enzymatic replication of the chromosomal origin of *Escherichia coli*. *Proc. Natl Acad. Sci. USA*, **81**, 424–428.
39. Wojtuszewski,K., Hawkins,M.E., Cole,J.L. and Mukerji,I. (2001) HU binding to DNA: evidence for multiple complex formation and DNA bending. *Biochemistry*, **40**, 2588–2598.
40. Koh,J., Saecker,R.M. and Record,M.T. Jr (2008) DNA binding mode transitions of *Escherichia coli* HU (alphabeta): evidence for formation of a bent DNA–protein complex on intact, linear duplex DNA. *J. Mol. Biol.*, **383**, 324–346.
41. Pinson,V., Takahashi,M. and Rouviere-Yaniv,J. (1999) Differential binding of the *Escherichia coli* HU, homodimeric forms and heterodimeric form to linear, gapped and cruciform DNA. *J. Mol. Biol.*, **287**, 485–497.
42. Bonnefoy,E., Takahashi,M. and Rouviere-Yaniv,J. (1994) DNA-binding parameters of the HU protein of *Escherichia coli* to cruciform DNA. *J. Mol. Biol.*, **242**, 116–129.
43. Pan,C.Q., Finkel,S.E., Cramton,S.E., Feng,J.A., Sigman,D.S. and Johnson,R.C. (1996) Variable structures of Fis-DNA complexes determined by flanking DNA-protein contacts. *J. Mol. Biol.*, **264**, 675–695.
44. Perkins-Balding,D., Dias,D.P. and Glasgow,A.C. (1997) Location, degree, and direction of DNA bending associated with the Hin recombinational enhancer sequence and Fis-enhancer complex. *J. Bacteriol.*, **179**, 4747–4753.
45. Thompson,J.F. and Landy,A. (1988) Empirical estimation of protein-induced DNA bending angles: applications to lambda site-specific recombination complexes. *Nucleic Acids Res.*, **16**, 9687–9705.
46. Stella,S., Cascio,D. and Johnson,R.C. (2010) The shape of the DNA minor groove directs binding by the DNA-bending protein Fis. *Genes Dev.*, **24**, 814–826.
47. Dorman,C.J. and Deighan,P. (2003) Regulation of gene expression by histone-like proteins in bacteria. *Curr. Opin. Genet. Dev.*, **13**, 179–184.
48. Shao,Y., Feldman-Cohen,L.S. and Osuna,R. (2008) Functional characterization of the *Escherichia coli* Fis-DNA binding sequence. *J. Mol. Biol.*, **376**, 771–785.
49. Finkel,S.E. and Johnson,R.C. (1992) The Fis protein: it's not just for DNA inversion anymore. *Mol. Microbiol.*, **6**, 3257–3265.
50. Smith,S.B., Finzi,L. and Bustamante,C. (1992) Direct mechanical measurements of the elasticity of single DNA molecules by using magnetic beads. *Science*, **258**, 1122–1126.
51. Strick,T.R., Allemand,J.F., Bensimon,D. and Croquette,V. (1998) Behavior of supercoiled DNA. *Biophys. J.*, **74**, 2016–2028.
52. Skoko,D., Li,M., Huang,Y., Mizuuchi,M., Cai,M., Bradley,C.M., Pease,P.J., Xiao,B., Marko,J.F., Craigie,R. *et al.* (2009) Barrier-to-autointegration factor (BAF) condenses DNA by looping. *Proc. Natl Acad. Sci. USA*, **106**, 16610–16615.
53. Yan,J., Maresca,T.J., Skoko,D., Adams,C.D., Xiao,B., Christensen,M.O., Heald,R. and Marko,J.F. (2007) Micromanipulation studies of chromatin fibers in *Xenopus* egg extracts reveal ATP-dependent chromatin assembly dynamics. *Mol. Biol. Cell*, **18**, 464–474.
54. Strick,T.R., Allemand,J.F., Bensimon,D., Bensimon,A. and Croquette,V. (1996) The elasticity of a single supercoiled DNA molecule. *Science*, **271**, 1835–1837.
55. Marko,J.F. and Siggia,E.D. (1995) Stretching DNA. *Macromolecules*, **28**, 8759–8770.
56. Yan,J., Kawamura,R. and Marko,J.F. (2005) Statistics of loop formation along double helix DNAs. *Phys. Rev. E Stat. Nonlin. Soft Matter Phys.*, **71**, 061905.
57. Zhang,H. and Marko,J.F. (2010) Intrinsic and force-generated cooperativity in a theory of DNA bending proteins. *Phys. Rev. E Stat. Nonlin. Soft Matter Phys.*, **82**, 051906.
58. Liebesny,P., Goyal,S., Dunlap,D., Family,F. and Finzi,L. (2010) Determination of the number of protein bound non-specifically to DNA. *J. Phys. Condens. Matter*, **22**, 414104.
59. Vladescu,I.D., McCauley,M.J., Nunez,M.E., Rouzina,I. and Williams,M.C. (2007) Quantifying force-dependent and zero-force DNA intercalation by single-molecule stretching. *Nat. Methods*, **4**, 517–522.
60. Hengen,P.N., Bartram,S.L., Stewart,L.E. and Schneider,T.D. (1997) Information analysis of Fis binding sites. *Nucleic Acids Res.*, **25**, 4994–5002.
61. Cho,B.K., Knight,E.M., Barrett,C.L. and Palsson,B.O. (2008) Genome-wide analysis of Fis binding in *Escherichia coli* indicates a causative role for A-/AT-tracts. *Genome Res.*, **18**, 900–910.
62. Kahramanoglou,C., Seshasayee,A.S., Prieto,A.I., Ibberson,D., Schmidt,S., Zimmermann,J., Benes,V., Fraser,G.M. and Luscombe,N.M. (2010) Direct and indirect effects of H-NS and Fis on global gene expression control in *Escherichia coli*. *Nucleic Acids Res.*, Advance Access Published on 21 November 2010; doi: 10.1093/nar/gkq934.
63. dos Remedios,C.G., Chhabra,D., Kekic,M., Dedova,I.V., Tsubakihara,M., Berry,D.A. and Nosworthy,N.J. (2003) Actin binding proteins: regulation of cytoskeletal microfilaments. *Physiol. Rev.*, **83**, 433–473.
64. Ferrer,J.M., Lee,H., Chen,J., Pelz,B., Nakamura,F., Kamm,R.D. and Lang,M.J. (2008) Measuring molecular rupture forces between single actin filaments and actin-binding proteins. *Proc. Natl Acad. Sci. USA*, **105**, 9221–9226.
65. Doyle,A.D. and Yamada,K.M. (2010) Cell biology: sensing tension. *Nature*, **466**, 192–193.
66. Geisler,M., Netz,R.R. and Hugel,T. (2010) Pulling a single polymer molecule off a substrate reveals the binding thermodynamics of cosolutes. *Angew. Chem. Int. Ed. Engl.*, **49**, 4730–4733.
67. Mosconi,F., Allemand,J.F., Bensimon,D. and Croquette,V. (2009) Measurement of the torque on a single stretched and twisted DNA using magnetic tweezers. *Phys. Rev. Lett.*, **102**, 078301.